A Comprehensive Investigation of Raman Laser-Induced Structural Modification in CVD-Grown Monolayer MoS_2

Sieun Jang[1], Seonha Park[1], Songkil Kim*[1]

1. Graduate School of Mechanical Engineering, Pusan National University

Busan, 609-735, Republic of Korea

** E-mail: songkil.kim@pusan.ac.kr*

ABSTRACT

Molybdenum disulfide (MoS_2), one of the most typical TMDCs, has been extensively explored to be utilized as electronic materials in a variety of device applications. Especially, the bandgap modulation of MoS_2 enables desirable properties, such as an appropriate direct bandgap, charge mobility, and on/off current ratio, making it a promising candidate for field-effect transistors (FETs). Moreover, the tunability of MoS_2 extends beyond electronic properties to include structural phase engineering. In this study, we irradiated a high-power Raman laser on the surface of chemical vapor deposition (CVD) monolayer MoS_2 under ambient conditions and thoroughly examined the modifications of the laser-induced spot according to the laser power and exposure time. We observed both etching and deposition phenomena in two discernible regions, and phase transition was found to be inhibited due to oxidation and the deposition of hydrogenated amorphous carbon.

KEY WORDS

CVD monolayer MoS_2, Raman laser irradiation, atomic force microscopy, structural modification, phase engineering.

1. INTRODUCTION

Two-dimensional (2D) nanomaterials possess unique properties due to their ultra-thin thickness.[1] In particular, the tunability of TMDCs renders them promising candidates as semiconducting materials to potentially replace silicon. Molybdenum disulfide (MoS_2), one of the most typical TMDCs, comprises stacked S-Mo-S monolayers. Bulk MoS_2 has an indirect bandgap of ~1.2 eV, which can be tuned to a direct bandgap but also refines the electrical properties of MoS_2. A single-layered MoS_2 exhibits high charge mobility (200~500 cm^2/V s) and a significant on/off current ratio (10^8), making it potential for field-effect transistors (FETs). The tunability of MoS_2 extends beyond electronic properties to include phase engineering relative to structural modulation. The structural transition from the semiconducting 2H phase to the metallic 1T phase can profoundly reduce the contact resistance (ranging from 0.7 kΩ μm to 10 kΩ μm) by eliminating the Schottky barrier and thereby establishing Ohmic contact between the MoS_2 and the metal electrode junction in MoS_2 field-effect transistor.[2,3] In this study, we irradiated high-power Raman laser on the surface of chemical vapor deposition (CVD) monolayer MoS_2 under ambient conditions and thoroughly examined the modifications of the laser-induced spot according to the laser power and exposure time by using atomic force microscopy (AFM) and Raman spectroscopy.

2. Result & Discussion

2.1 Raman laser-induced structural modification in monolayer MoS_2

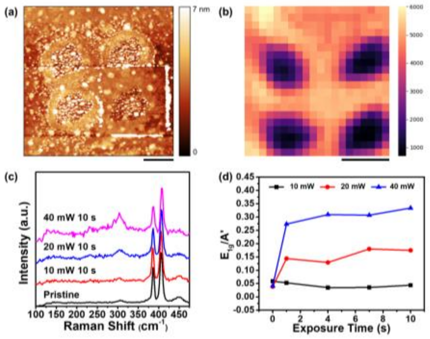

Fig.l: (a) Atomic force microscopy (AFM) topography image of the laser spot with part of the area scratched. (b) Raman intensity mapping image of (b) at A' vibration mode. (c) Raman spectra of the center of the laser spot according to the power. (d) The Raman peak ratio of the E_{1g}/A' according to the laser power and exposure time.

We irradiated a Raman laser on the surface of a CVD monolayer MoS_2 on SiO_2/Si substrate under ambient conditions, varying the power and the exposure time. Figure 1(a) shows the AFM topography images, where one spot was scratched with an AFM probe while the others were left intact. Two distinct morphologies were observed within the laser spot, which can be divided into outer and inner regions based on their distance from the center. The outer region of the laser spot exhibits an approximate thickness of 2 nm, which seems to be the deposition on the MoS_2 surface. In contrast, the core of the exposed area displayed the formation of thickly stacked substances. Figure 1(b) shows the intensity mapping image of Figure 1(a) at A' (~405 cm^{-1}) vibration mode which indicates the 2H phase of MoS_2. The decreasing intensity toward the center reflects the laser-irradiated region, which has a similar size to the etching area of MoS_2, approximately ~1 μm. We can assume that the dark region of the mapping image demonstrates the etching area of MoS_2. By the way, after the one spot scratching, no dimensional reduction was observed in the dark area of the mapping image despite the removal of the deposits. This unchanged 2H phase signal suggests that the deposits are unrelated to the etching and the phase transition of MoS_2.

The further explore these effects, Raman measurements were conducted according to the laser power, particularly focused on the core area of the laser spot, as shown in Figure 1(c). In the spectra, most of them exhibited the peak positions of the E' (~385 cm^{-1}) and A' vibration modes, indicating the 2H phase of monolayer MoS_2. These peaks are attributed to the spatial dimensions of the laser affecting the nearby 2H phase of MoS_2. Other peaks within the range of 100~350 cm^{-1}, marked as the blue box, correspond to the SiO_2/Si substrate, including the E_{1g} peak which is the most prominent feature of the SiO_2/Si substrate. At a power of 10 mW, the spectra of the laser spot center and pristine MoS_2 are similar; conversely, at 20 and 40 mW, the SiO_2/Si substrate peaks significantly increased after Raman laser irradiation. This increase in SiO_2/Si substrate peaks implies that MoS_2 has been etched, yet the height profile of the AFM image shows an increase in the center area compared to pristine MoS_2.

Figure 1(d) shows the trend of the accurate peak ratio of E_{1g}/A' as a function of laser power and exposure time. While the extent of the etching of MoS_2 increased with laser power, the ratio reached saturation with respect to the exposure time. Thus, an exposure time of 1 second might be sufficient to alter MoS_2 at each laser power, and the continuous deposition in the outer region prevented MoS_2 from being etched further into the peripheral area. It is assumed that the etching of MoS_2 occurs more rapidly than the phase transition from the 2H phase to the 1T phase due to oxidation, and both etching and deposition during laser irradiation inhibit the phase transformation.

2.2 Unveiling the underlying mechanism of Raman laser irradiation on monolayer MoS_2

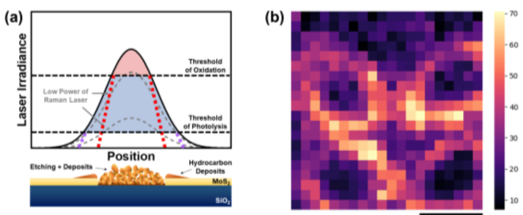

Fig.2: (a) Schematic illustration depicting the effects on monolayer MoS_2 relative to the spatial distribution of the laser intensity and its interaction with the sample. (b) Raman intensity mapping image at the hydrogenated amorphous carbon (a:C-H) peak. The scale bar represent 1 μm.

To find out the characteristics of the deposit, another intensity mapping of Figure 1(a) was analyzed at the hydrogenated amorphous carbon (a-C:H) peak (Figure 2(b)). The peaks of hydrogenated amorphous carbon generally have two broad D (~1392 cm^{-1}) and G (~1576 cm^{-1}) peaks. In the Raman mapping image, it is worth noting that hydrogenated amorphous carbon shows high intensity according to the morphology of deposits in the outer region of the laser spot. Moreover, the peak of hydrogenated amorphous carbon was also present in the center of the laser spot although the intensity was relatively low. It is proposed that the a-C:H is deposited both on the center and peripheral area of the laser spot.

Given all the preceding discussions, the effect of laser irradiation on monolayer MoS_2 under ambient conditions can be understood through the schematic in Figure 2(a). The Raman laser follows a Gaussian intensity distribution, meaning that the intensity diminishes progressively from the center to the outer region. At this point, two disparate intensity thresholds were established, each corresponding to a unique morphology within the spot, based on the spatial distribution of laser irradiance. We suggest that the higher threshold is associated with the etching process, while the lower threshold corresponds to the deposition process. When the irradiance exceeds the lower threshold, a-C:H is deposited both in the center and outer regions of the laser spot. We suggest that it can be attributed to the photolysis of hydrocarbon present in the air.

3. Conclusion

In conclusion, we observed the effects of Raman laser irradiation on CVD monolayer MoS_2 under ambient conditions, with the power from 10 to 40 mW and the exposure time from 1 to 10 s, to explore the underlying mechanism of MoS_2-laser interaction and subsequent modifications. Following the Gaussian distribution laser, the morphology of the laser spot reveals two discernible regions based on the concentricity from the center of the laser spot. In the outer region, hydrogenated amorphous carbon was deposited on the monolayer MoS_2, in comparison, etching and deposition coincide in the inner region of the laser spot. As a result, the etching of MoS_2 proceeds more rapidly than the phase transition from the 2H phase to the 1T phase due to oxidation and hydrogenated amorphous carbon deposition, therefore, the phase transition is impossible using laser irradiation in ambient conditions.

ACKNOWLEDGEMENTS

This research was primarily supported by the National Research Foundation of Korea (NRF) grant funded by the Korea government (MSIT) (No. 2022R1A2C2012472) and partially supported by the PNU Hybrid Innovation Manufacturing Engineering Center (No. 2021R1A6C101A449)

REFERENCES

1 U. Krishnan *et al.*, *Superlattices Microstruct.*, 128 (2019) 274~297.
2 R. Kappera *et al.*, *Nature. Mater.* 13 (2014) 1128~1134.
3 G. Eda *et al.*, *ACS Nano*, 6 (2012) 7311~7317.